Purinergic Signalling (2018) 14:19–26
https://doi.org/10.1007/s11302-017-9589-9

ORIGINAL ARTICLE

Myeloid P2Y2 receptor promotes acute inflammation but is dispensable for chronic high-fat diet-induced metabolic dysfunction

Samantha E. Adamson[1,2] · **Garren Montgomery**[1] · **Scott A. Seaman**[2,3] · **Shayn M. Peirce-Cottler**[2,3] · **Norbert Leitinger**[1,2]

Received: 20 September 2016 / Accepted: 10 October 2017 / Published online: 30 October 2017
© Springer Science+Business Media B.V. 2017

Abstract The purinergic receptor P2Y2 binds ATP to control chemotaxis of myeloid cells, and global P2Y2 receptor knockout mice are protected in models of acute inflammation. Chronic inflammation mediated by macrophages and other immune cells in adipose tissue contributes to the development of insulin resistance. Here, we investigate whether mice lacking P2Y2 receptors on myeloid cells are protected against acute and chronic inflammation. Wild-type mice were transplanted with either wild-type or P2Y2 receptor null bone marrow and treated with a sublethal dose of endotoxin as a model of acute inflammation, or fed a high-fat diet to induce obesity and insulin resistance as a model of chronic inflammation. $P2Y2^{-/-}$ chimeric mice were protected against acute inflammation. However, high-fat diet feeding induced comparable inflammation and insulin resistance in both WT and $P2Y2^{-/-}$ chimeric mice. Of note, confocal microscopy revealed significantly fewer crown-like structures, assemblies of macrophages around adipocytes, in $P2Y2^{-/-}$ chimeric mice compared to WT chimeric mice. We conclude that P2Y2 receptors on myeloid cells are important in mediating acute inflammation but are dispensable for the development of whole body insulin resistance in diet-induced obese mice.

Keywords P2Y2 receptor · Bone marrow transplant · Myeloid · Endotoxemia · Insulin resistance

Electronic supplementary material The online version of this article (https://doi.org/10.1007/s11302-017-9589-9) contains supplementary material, which is available to authorized users.

✉ Norbert Leitinger
nl2q@virginia.edu

[1] Department of Pharmacology, University of Virginia, PO Box 800735, Charlottesville, VA 22908, USA

[2] Cardiovascular Research Center, University of Virginia, Charlottesville, VA 22908, USA

[3] Department of Biomedical Engineering, University of Virginia, Charlottesville, VA 22908, USA

Introduction

The purinergic P2Y2 receptor (P2ry2) is a G-protein-coupled receptor that binds ATP and mediates several aspects of immune cell function including chemotaxis [1–3]. P2Y2 receptor null mice are protected in models of acute inflammation due to decreased leukocyte recruitment [4, 5]. In macrophages, purinergic signaling controls chemotactic, phagocytic, and inflammatory responses [6]. Moreover, activation of P2Y2 receptors on macrophages during inflammatory challenge contributes to expression of inflammatory mediators including cyclo-oxygenase 2 and inducible nitric oxide synthase, and the expression of *P2ry2* messenger RNA (mRNA) was increased in cultured macrophages treated with lipopolysaccharide (LPS) [7]. P2Y2 receptors also sense extracellular ATP that is released from apoptotic cells by pannexin 1 channels [8, 9], to control macrophage migration and inflammation [10].

In addition to acute inflammation, several purinergic receptors have been shown to play a role in diseases with a chronic inflammatory component such as atherosclerosis and diabetes [11, 12]. During obesity, immune cell infiltration of adipose tissue produces inflammation which contributes to insulin resistance [13], and preventing macrophage infiltration into adipose tissue decreases inflammation and insulin resistance [14, 15]. Inflammasome-mediated inflammation within adipose tissue contributes to insulin resistance [16, 17]; however, a recent study ruled out inflammasome activation via the purinergic receptor P2X7 in the development of diet-induced insulin resistance [18].

The purpose of this study was to investigate the role of myeloid P2Y2 receptor in chronic inflammation in a model of diet-induced obesity and insulin resistance compared to the role of myeloid P2Y2 receptor during acute inflammation in a model of sublethal endotoxemia. To this end, we generated WT and $P2Y2^{-/-}$ chimeric mice (WT-tp and $P2Y2^{-/-}$-tp) by transplanting wild-type mice with either wild-type or P2Y2 receptor null bone marrow. Acute inflammatory challenge with LPS showed that $P2Y2^{-/-}$ chimeric mice were partially protected against inflammation. On the other hand, high-fat diet challenge of WT and $P2Y2^{-/-}$ chimeric mice resulted in similar levels of adipose tissue inflammation and systemic insulin resistance between groups.

Methods

Mice All animal studies were approved by the Animal Care and Use Committee at the University of Virginia. Female mice were used for all studies. Bone marrow transplantation was performed as described previously [19, 20]. Briefly, 4-week-old recipient C57Bl/6 mice received 80 mg/mL sulfmethoxazole and 0.37 mM trimethoprim in autoclaved water 6 days prior to receiving two doses of 600 RAD each, 4 h apart (Shepard Mark irradiator). Bone marrow was harvested from tibias and femurs of donor WT (C57Bl/6) and global $P2Y2^{-/-}$ mice [8] (kindly provided by Dr. Kodi Ravichandran, University of Virginia), and two million bone marrow cells were given to each recipient mouse by tail vein injection. Recipient mice were maintained on antibiotics (80 mg/mL sulfmethoxazole and 0.37 mM trimethoprim in autoclaved water) for 4 weeks to protect them from infection. Further experiments described below were begun after a total of 6 weeks post irradiation and transplantation to give sufficient time for reconstitution. Bone marrow-derived macrophages were cultured for 7 days in RPMI media supplemented with 1% antibiotics, 10% FBS, and M-CSF-rich supernatant from L929 cells as previously described [21, 22].

Endotoxemia was induced by i.p. injection of 2 mg/kg lipopolysaccharide (LPS *Escherichia coli* 0111:B4) for 24 h [21, 22]. Blood was taken by tail bleeding at indicated time points and spun down for serum cytokine analysis by ELISA (BioLegend). Peripheral whole blood was taken from the tails of mice and analyzed by Hemavet (Drew Scientific).

Mice were fed a high-fat diet containing 60% cal from fat and 0.2% cholesterol (Bio-Serv) or normal chow (Teklad). Mice were weighed weekly. Food intake was determined by measuring the difference in food weight over a period of days. Fat and lean masses were measured by DEXA scan. Glucose tolerance tests were performed as described [19, 22] in accordance with recommendations published by Ayala et al. [23]. For glucose tolerance test, mice were fasted for 6 h and then injected with 1 g/kg glucose i.p. and blood glucose levels were measured from tail blood by glucometer (OneTouch Ultra) over 2 h. Area under the curve (AUC) was determined by setting baseline to time 0 value. Serum cytokines and insulin levels were determined by ELISA (BioLegend and CrystalChem, respectively). Adipocytes and stromal vascular fraction cells were isolated from murine perigonadal adipose tissue by mincing and collagenase digestion followed by washing in Krebs-Ringer-HEPES-BSA buffer. Adipocytes were floated, and infranatant containing stromal vascular fraction (SVF) cells was collected with a long blunted needle followed by centrifugation at 1500 rpm for 5 min at 4 °C to pellet cells which were resuspended in 0.83% ammonium chloride for 10 min to lyse red blood cells. SVF cells were counted by hemocytometer and normalized to grams of adipose tissue processed.

Confocal microscopy For whole mount staining of adipose tissue, perigonadal fat pad samples were harvested and permeabilized by submersion in 0.2% saponin/PBS solution overnight at 4 °C. Samples were submerged in a 5 μg/mL solution of BODIPY 493/503 for 15 min at 37 °C in the dark. Following washing with PBS, samples were blocked in 0.2% saponin/PBS/5% goat serum. The samples were then incubated overnight in the dark in 0.2% saponin/PBS/5% goat serum containing preconjugated Alexa Fluor 647 CD68 (1:300) to detect macrophages. Tissue samples were washed three times for 5 min in 0.2% saponin/PBS. Alexa Fluor 568 goat anti-rabbit (1:300) in 0.2% saponin/PBS was applied for 2 h at room temperature followed by six 5-min washes. Samples were mounted on gelatin-coated microscope slides using 50:50 PBS/glycerol solution. Using a Nikon TE 2002-E2 microscope, a Melles Griot Argon Ion Laser System, and a confocal attachment, digital confocal images of the stained samples were acquired for later analysis. Crown-like structures clearly visible as CD68-positive cells assembling around an adipocyte [24, 25] were quantified by three independent and blinded observers.

Isolation of RNA and real-time PCR RNA isolation was performed using RLT buffer (Qiagen RNA Blood Mini Kit) and then purified using RNeasy columns (Qiagen), followed by quantification and purification analysis with NanoDrop (Thermo). Complementary DNA (cDNA) was synthesized from 250 μg total RNA with an iScript cDNA synthesis kit (Bio-Rad) according to the manufacturer's instructions. For real-time PCR, synthesized cDNA forward and reverse primers along with SYBR GreenER (Invitrogen) master mix were run on the CFX Connect Real-Time System. β-2-Microglobin was used as an internal control.

Gene name	Forward primer sequence	Reverse primer sequence
P2yr2	TTTGTGGCTTACAG CTCCGT	CCTCCTGTGGTCCC ATAAGC

Nos2	TGTTAGAGACACTT CTGAGGCTC	CACTTTGGTAGGAT TTGACTTT
Arg1	AAGACAGCAGAGGA GGTGAAGAG	TGGGAGGAGAAGGC GTTTGC
Il6	CCACGGCCTTCCCT ACTTCA	TGCAAGTGCATCAT CGTTGTTC
Tnfα	GAACTGGCAGAAGA GGCACT	AGGGTCTGGGCCAT AGAACT
IL1β	TACCAGTTGGGGAA CTCTGC	CAAAATACCTGTGG CCTTGG
Il10	CCAAGGTGTCTACAAGGC	TAGAATGGGAACTG AGGTATC
β2M	GCTATCCAGAAAAC CCCTCAAATTCA	GCAGGCGTATGTAT CAGTCTCAGTG

Statistical analysis Statistical analyses were performed with GraphPad Prism (GraphPad, San Diego, CA). Student's *t* test or ANOVA with post hoc comparison tests were used as appropriate. *F* test was performed in Prism to determine if variances were similar among groups.

Results

P2Y2$^{-/-}$-tp mice challenged acutely with LPS are protected from inflammation

To study the role of P2Y2 receptor specifically on myeloid cells during inflammation, we transplanted C57Bl/6 mice with bone marrow isolated from WT or global P2Y2$^{-/-}$ mice [8] to obtain WT chimeric (WT-tp) mice and P2Y2$^{-/-}$ chimeric mice (P2Y2$^{-/-}$-tp). Measuring *P2y2r* mRNA from blood from WT-tp and P2Y2$^{-/-}$-tp mice demonstrated significantly decreased *P2y2r* mRNA levels in blood from P2Y2$^{-/-}$-tp mice compared to WT-tp mice (Fig. 1a), confirming successful bone marrow transplantation. *P2y2r* expression was sensitive to the gram-negative bacterial wall component lipopolysaccharide (LPS), since acute challenge of WT-tp mice with a sublethal dose of LPS intraperitoneally resulted in significantly increased expression of *P2y2r* mRNA levels in blood (Fig. 1b), supporting previously published observations that in vitro treatment of macrophages with LPS increased *P2y2r* mRNA [7]. When WT-tp and P2Y2$^{-/-}$-tp mice were challenged intraperitoneally with either saline (SAL) or a sublethal dose of LPS for 24 h, we observed significantly lower levels of the cytokines interleukin-6 (IL6) and tumor necrosis factor alpha (TNFα) in the serum from P2Y2$^{-/-}$-tp mice compared to WT-tp mice (Fig. 1c). In that context, global P2Y2 receptor knockout mice have been reported to have increased survival compared to wild-type mice in a model of mouse sepsis, which is thought to be due to a decrease in leukocyte recruitment [4]. To examine a possible defect in leukocyte emigration from the bone marrow in response to LPS, we analyzed blood from saline and LPS-treated WT-tp and P2Y2$^{-/-}$-tp mice for absolute numbers of neutrophils (NEs), lymphocytes (LYs), and monocytes (MOs) as well as their relative abundance. We found that LPS treatment significantly increased the relative abundance of NEs and significantly decreased the absolute number and percentage of lymphocyte (LYs) and the absolute number of monocytes in blood, but there was no significant difference between WT-tp and P2Y2$^{-/-}$-tp mice in the saline-treated or LPS-treated condition (Fig. 1d). The mRNA expression of chemokines *Cxcl1* and *Cxcl2* were not significantly different in WT and P2Y2-deficient bone marrow-derived macrophages treated with ATP or UTP (Supplementary Fig. 1A), indicating that chemokine expression is not directly regulated by the P2Y2 receptor. Taken together, these results indicate that P2Y2 receptors on myeloid cells play a role in controlling inflammatory gene expression during endotoxemia.

Regulation of the arginine pathway by myeloid P2Y2 receptors during acute inflammation

To further investigate myeloid cell-intrinsic mechanisms involved in the regulation of inflammation by P2Y2 during acute challenge, we isolated peritoneal cells from WT-tp and P2Y2$^{-/-}$-tp mice treated with LPS for 24 h and measured mRNA levels of inflammatory and anti-inflammatory genes including inducible nitric oxide synthase (*Nos2*), arginase 1 (*Arg1*), interleukin 6 (*Il6*), tumor necrosis factor alpha (*Tnfα*), interleukin 1-beta (*Il1β*), and interleukin 10 (*Il10*). Peritoneal cells from LPS-treated P2Y2$^{-/-}$-tp mice had significantly decreased levels of *Nos2* and *Arg1* mRNA compared to WT-tp mice, but had equivalent levels of all other cytokines measured (Fig. 2a). Previously, activation of P2Y2 receptors has been shown to upregulate *Nos2* expression in macrophages [7, 26]. When bone marrow-derived macrophages from WT and P2Y2 receptor null mice were treated with 1 μg/mL LPS for 6 h, we observed significantly decreased *Nos2* mRNA levels in P2Y2 receptor null macrophages (Fig. 2b). Taken together, this data suggests that the absence of P2Y2 receptor specifically on myeloid cells is protective during acute inflammation by altering the expression of enzymes involved in arginine metabolism.

Myeloid P2Y2 receptor deficiency does not alter weight gain, adiposity, or food intake during high-fat diet challenge

During obesity, chronic immune cell infiltration into adipose tissue was shown to contribute to the development of insulin resistance [13]. To determine whether P2Y2 receptors on myeloid cells play a role in obesity-associated chronic inflammation, we fed WT-tp and P2Y2$^{-/-}$-tp mice a high-fat diet (HFD) (60% kcal from fat) or control chow diet for up to 20 weeks. High-fat diet feeding significantly increased weight gain in

WT-tp and P2Y2$^{-/-}$-tp mice compared to chow diet-fed mice ($p < 0.0001$), but there was no difference in weight between WT-tp and P2Y2$^{-/-}$-tp mice (Fig. 3a). Adiposity measured by DEXA scan was equivalent between high-fat diet-fed WT-tp and P2Y2$^{-/-}$-tp mice (Fig. 3b), as was food intake (Fig. 3c). Peripheral blood from WT-tp and P2Y2$^{-/-}$-tp mice fed chow or high-fat diet for 12 weeks was analyzed for absolute numbers of NEs, LYs, and MOs as well as their relative abundance (Fig. 3d). The relative abundance of peripheral blood neutrophils was increased, while the relative abundance of lymphocytes was decreased in mice fed high-fat diet compared to chow; however, there was no difference between WT-tp and P2Y2$^{-/-}$-tp mice (Fig. 3d). These results demonstrate that deficiency of myeloid P2Y2 receptor does not alter weight gain, adiposity, or food intake during high-fat diet challenge.

Systemic and adipose tissue inflammation of high-fat diet-fed P2Y2$^{-/-}$-tp mice is comparable to WT-tp mice, yet macrophage crown-like structure formation is significantly reduced

High-fat-fed WT-tp and P2Y2$^{-/-}$-tp mice showed no difference in levels of serum cytokines including TNFα, IL6, and IL10 (Fig. 4a). During obesity, immune cell infiltration of adipose tissue produces inflammation which contributes to insulin resistance [13]. Macrophages assemble around dying adipocytes, forming what are termed crown-like structures (CLSs) [24]. Confocal microscopy of perigonadal adipose tissue from high-fat diet-fed WT-tp and P2Y2$^{-/-}$-tp mice was performed to identify macrophages, which were observed to surround adipocytes to form CLS in adipose tissue from WT-tp mice, while these readily identifiable structures were rarely detected in adipose tissue from P2Y2$^{-/-}$-tp mice. Quantification of CLS showed that after 12 weeks of high-fat diet feeding, CLSs were frequently observed in WT-tp adipose tissue, but no CLSs were observed in adipose tissue from P2Y2$^{-/-}$-tp (Fig. 4b). By 20 weeks of high-fat diet feeding, CLSs were increased in adipose tissue from both P2Y2$^{-/-}$-tp and WT-tp mice, but the number of CLS in adipose tissue from WT-tp mice was lower (Fig. 4b). The difference in the presence of CLS was independent of overall immune cell infiltration into the adipose tissue as equivalent numbers of cells in the SVF, which include macrophages and other immune cells, were observed in perigonadal adipose tissue from WT-tp and P2Y2$^{-/-}$-tp mice (Fig. 4c). Additionally, there was no difference in adipocyte size between high-fat diet-fed WT-tp and P2Y2$^{-/-}$-tp

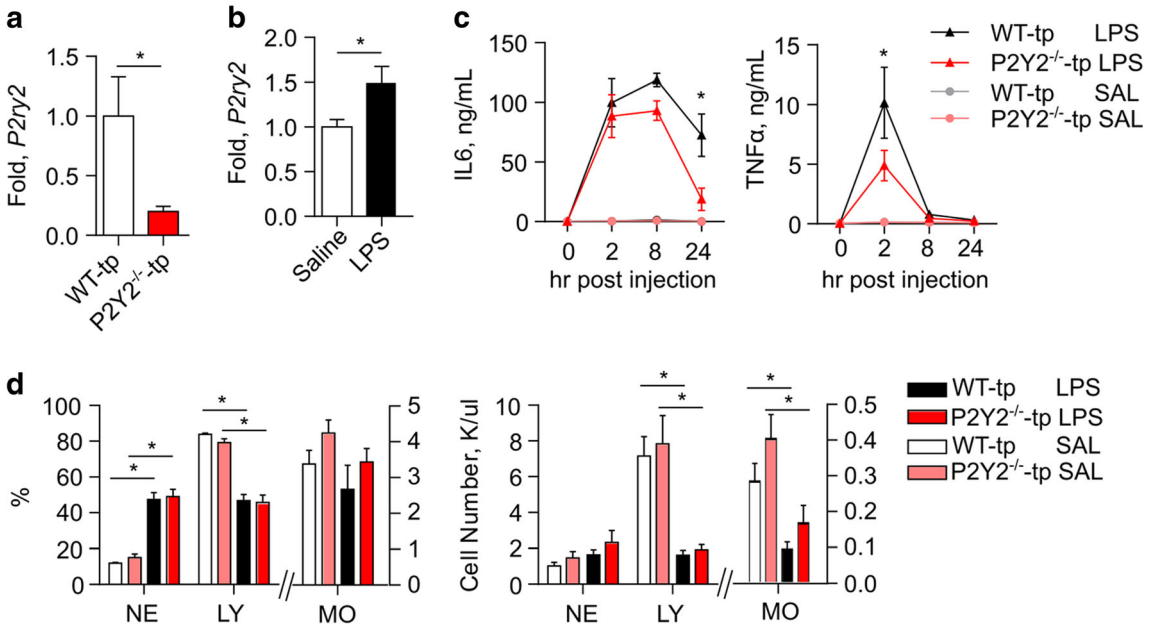

Fig. 1 P2Y2$^{-/-}$-tp mice challenged acutely with LPS are protected from inflammation. *P2y2r* mRNA levels in blood of WT-tp and P2Y2$^{-/-}$-tp mice were measured by qRT-PCR and revealed a significant decrease in the mice transplanted with P2Y2 null marrow ($N = 12$, mean ± SEM, $p < 0.006$ by Mann-Whitney test) (**a**). WT-tp and P2Y2$^{-/-}$-tp mice were dosed i.p. with either saline or 2 mg/kg LPS for 24 h (**b–d**). Expression of *P2y2r* mRNA was measured in blood from WT-tp mice and normalized to B2M revealing a significant increase in *P2y2r* mRNA upon LPS treatment ($N = 5$, mean ± SEM, $p < 0.05$ by Student's *t* test) (**b**). Serum IL6 and TNFα levels were measured by ELISA over the 24-h period. P2Y2$^{-/-}$-tp mice have significantly lower serum IL6 at 24 h and significantly lower TNFα at 2 h ($N = 6$, mean ± SEM, $p < 0.0001$ by two-way repeated measures ANOVA with Tukey's multiple comparison test) (**c**). Hemavet analysis of immune cells from blood reveals no difference in immune cell distribution or absolute number between WT and P2Y2$^{-/-}$-tp mice after 24 h of LPS treatment ($N = 6$, mean ± SEM), *$p < 0.001$ by two-way ANOVA with Tukey's multiple comparison test (**d**)

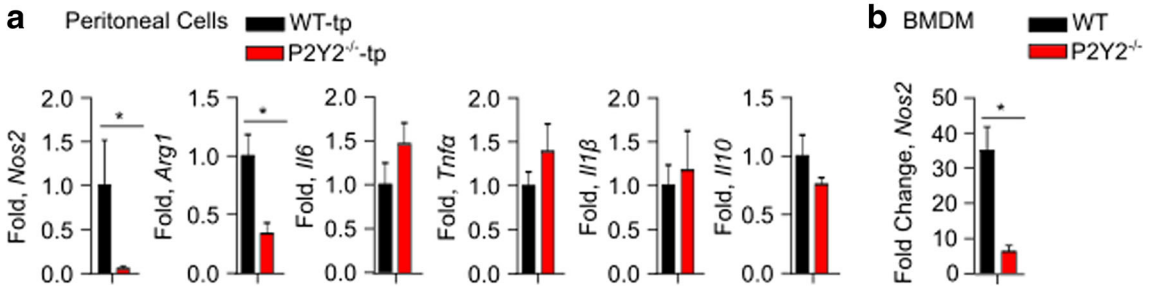

Fig. 2 Regulation of arginine metabolic pathway by myeloid P2Y2 receptor during acute inflammation. **a** WT-tp and P2Y2$^{-/-}$-tp mice were dosed i.p. with 2 mg/kg LPS for 24 h, and peritoneal lavage was performed. mRNA levels of nitric oxide synthase (*Nos2*), arginase 1 (*Arg1*), interleukin 6 (*Il6*), tumor necrosis factor alpha (*Tnfα*), interleukin 1-beta (*Il1β*), and interleukin 10 (*Il10*) were determined by qRT-PCR. Data is normalized to β2-microglobulin mRNA and expressed as mean ± SEM, *$p < 0.01$ by unpaired, two-tailed Student's *t* test. **b** Bone marrow-derived macrophages were obtained from WT and P2Y2 receptor null mice and treated with 1 μg/mL LPS for 6 h. Experiment was performed in quadruplicate. Data is normalized to β2-microglobulin mRNA and expressed as fold change from untreated control, mean ± SEM, *$p = 0.02$ by unpaired, two-tailed Student's *t* test with Welch's correction

mice (Fig. 4d). To further investigate the inflammatory status of adipose tissue in high-fat diet-fed WT-tp and P2Y2$^{-/-}$-tp mice, we analyzed the expression of cytokines including *Il6*, *Tnfα*, and *Il1β* and enzymes *Nos2* and *Arg1*. While the expression of both *Il6* and *Tnfα* was comparable in WT-tp and P2Y2$^{-/-}$-tp mice, expression of *Il1β* mRNA tended to be increased in adipose tissue from P2Y2$^{-/-}$-tp mice, but the difference did not reach statistical significance (Fig. 4e). *Arg1* mRNA levels showed a statistically insignificant decrease in P2Y2$^{-/-}$-tp mice, and there was no difference in *Nos2* mRNA levels (Fig. 4e). Together, we found that neither systemic cytokine levels nor adipose tissue inflammation and immune cell content appeared different between high-fat diet-fed WT-tp and P2Y2$^{-/-}$-tp mice; however, adipose tissue of high-fat diet P2Y2$^{-/-}$-tp mice appeared to contain significantly fewer crown-like structures, which may be attributed to a migration defect of P2Y2-deficient macrophages towards dying adipocytes [8].

Insulin resistance develops equally in high-fat diet-fed WT-tp and P2Y2$^{-/-}$-tp mice

Serum insulin levels were increased in both WT-tp and P2Y2$^{-/-}$-tp mice upon high-fat diet feeding, with no

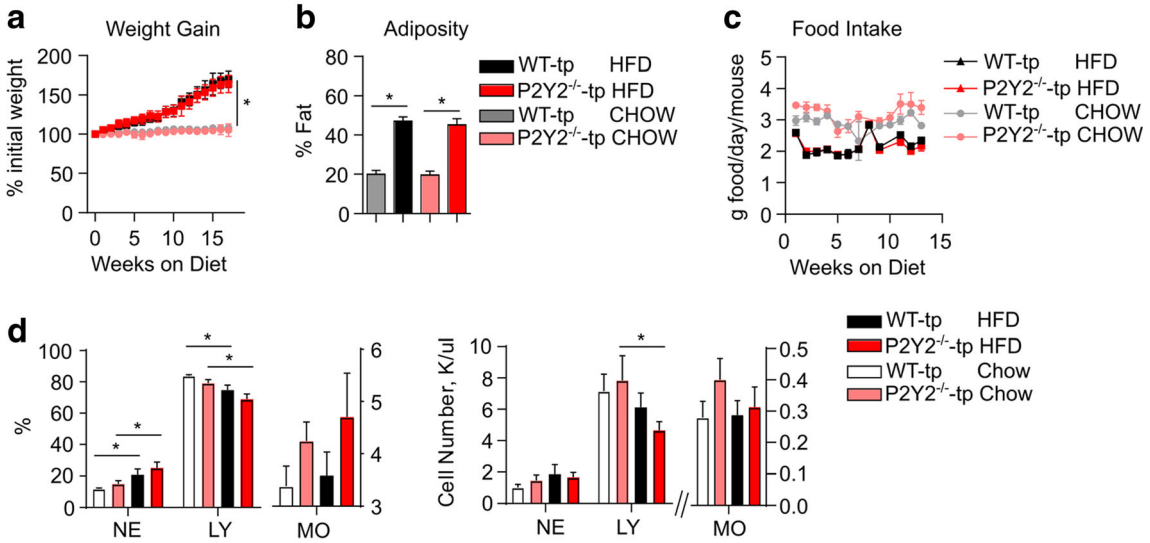

Fig. 3 Myeloid P2Y2 receptor deficiency does not alter weight gain, adiposity, or food intake during high-fat diet challenge. WT-tp and P2Y2$^{-/-}$-tp mice were fed either a regular chow diet (Teklad) or high-fat diet (60% kcal from fat with 0.2% cholesterol, Bio-Serv) for up to 20 weeks. Mice were weighed weekly to reveal no difference between WT-tp and P2Y2$^{-/-}$-tp mice weight gain on high-fat diet ($N = 12$, mean ± SD), *$p < 0.0001$ by two-way ANOVA (**a**). Adiposity was determined for WT-tp and P2Y2$^{-/-}$-tp mice after 17 weeks of diet by DEXA scan ($N = 12$, mean ± SD, $p < 0.0001$ by one-way ANOVA with Sidak's multiple comparison test) (**b**). Food intake was determined for WT-tp and P2Y2$^{-/-}$-tp mice by determining food weight weekly per cage of four mice ($N = 3$ cages of 4 mice, mean ± SEM) (**c**). Hemavet analysis of blood immune cell distribution and absolute number from WT and P2Y2$^{-/-}$-tp mice fed either chow or high-fat diet for 12 weeks ($N = 4$, mean ± SEM), *$p < 0.001$ by two-way ANOVA with Tukey's multiple comparison test (**d**)

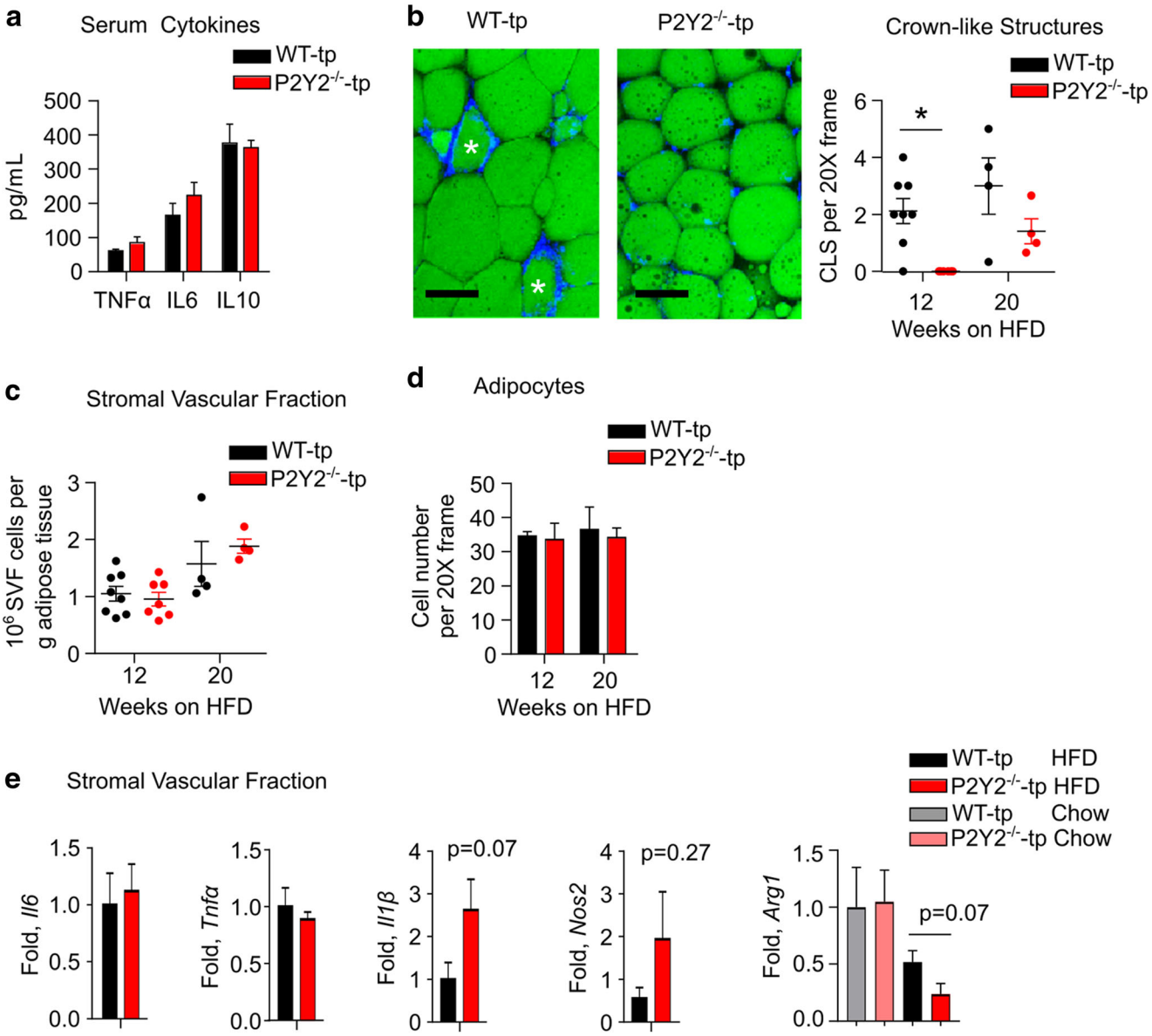

Fig. 4 Myeloid P2Y2 receptor does not contribute to overall inflammation during high-fat diet challenge, but may alter macrophage migration within adipose tissue. Serum TNFα, IL6, and IL10 levels were measured by ELISA in WT-tp and P2Y2$^{-/-}$-tp mice after 10 weeks on high-fat diet (N = 6–7, mean ± SEM) (**a**). Whole mount staining of perigonadal adipose tissue from WT-tp and P2Y2$^{-/-}$-tp mice after 12 and 20 weeks on high-fat diet with the macrophage marker CD68 was analyzed by confocal microscopy, and crown-like structures were quantified. Representative images are shown from mice fed high-fat diet for 12 weeks. Bodipy staining in green and CD68 in blue. Scale bar (black) represents 40 μm. Two CLSs denoted with white asterisks in left panel. Three ×20 images were quantified per mouse and averaged by three independent observers. Each point represents one mouse. Data presented as mean ± SEM. *p = 0.0037 by Mann-Whitney test for data at 12 weeks (**b**). Stromal vascular cells isolated from perigonadal adipose tissue from WT-tp and P2Y2$^{-/-}$-tp mice after 12 and 20 weeks on high-fat diet were quantified by hemocytomer. Each point represents one mouse. Data presented as mean ± SEM (**c**). Adipocyte number was quantified from histologic sections of adipose tissue from WT-tp and P2Y2$^{-/-}$-tp mice after 12 and 20 weeks on high-fat diet. N = 6–8 mice at 12 weeks, N = 4 mice at 20 weeks. Three sections analyzed per mouse by three separate blinded investigators and results averaged. Data presented as mean ± SEM (**d**). mRNA levels of cytokines including *Il6*, *Tnfα*, and *Il1β* and enzymes *Nos2* and *Arg1* were measured by qRT-PCR in stromal vascular cells isolated from perigonadal adipose tissue from WT-tp and P2Y2$^{-/-}$-tp mice after 12 weeks on high-fat diet. Data is normalized to β2-microglobulin mRNA and expressed as mean ± SEM (N = 6–7). Data was analyzed by unpaired, two-tailed Student's t test, p values as shown (**e**)

significant difference between groups (Fig. 5a). Glucose tolerance tests revealed that high-fat diet feeding decreased glucose tolerance at 10 weeks, but there was no difference between WT-tp and P2Y2$^{-/-}$-tp mice (Fig. 5b). Taken together, this data demonstrates that the P2Y2 receptor on myeloid cells is dispensable for diet-induced insulin resistance in mice.

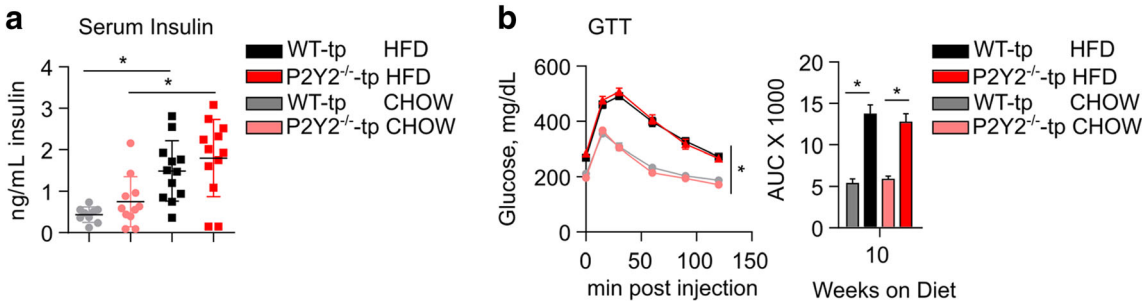

Fig. 5 Insulin resistance is equivocal in high-fat diet-fed WT-tp and P2Y2$^{-/-}$-tp mice. Insulin levels were measured by ELISA in serum obtained from 6 h fasted WT-tp and P2Y2$^{-/-}$-tp mice after 10 weeks on diet. (N = 9–12, each point represents one mouse, mean ± SD, *p < 0.01 by Student's t test, two-tailed) (**a**). Whole body glucose tolerance was assessed by glucose tolerance test in which mice were fasted for 6 h and then dosed intraperitoneally with 2 g/kg glucose in saline. Blood glucose was measured by handheld glucometer (OneTouch Ultra) for up to 2 h. Blood glucose curve is shown for glucose tolerance test performed after 10 weeks on diet. (N = 11–12, mean ± SEM, *p < 0.0001 by two-way ANOVA). Quantification of area under the curve is shown at the right for glucose tolerance tests performed after 10 weeks of diet. (N = 11–12, mean ± SEM, *p < 0.0001 by one-way ANOVA with Sidak's multiple comparison test (**b**)

Discussion

The purpose of this study was to investigate the role of myeloid P2Y2 receptor in acute inflammation in a model of sublethal endotoxin dosed intraperitoneally and chronic inflammation in a model of diet-induced obesity and insulin resistance. In line with previous studies [4, 5], we have shown that P2Y2 receptor deficiency results in decreased inflammation upon acute challenge with lipopolysaccharide. Specifically, our study demonstrates a role for P2Y2 receptors on myeloid cells. We also found that LPS treatment increased *P2y2r* mRNA in vivo, supporting previous in vitro studies [7]. We did not find an effect of P2Y2 deficiency on leukocyte mobilization from bone marrow in response to LPS; however, LPS-induced iNOS and arginase 1 expression were dependent on the presence of P2Y2 receptors on macrophages. Inducible nitric oxide synthase metabolizes arginine to nitric oxide and citrulline, while arginase 1 metabolizes arginine to ornithine and urea [27, 28]. It has been suggested that arginine is differentially metabolized during the inflammatory response: initially, arginine is metabolized by iNOS to produce nitric oxide which is a critical regulator of proinflammatory cytokine expression [29]; later, arginine is metabolized by arginase to produce compounds critical for tissue repair [28]. Our data suggests that P2Y2 receptors specifically on myeloid cells are involved in the regulation of acute inflammation by altering the expression of enzymes involved in arginine metabolism.

While the absence of P2Y2 receptors on myeloid at least partially protected mice from LPS-induced acute inflammation, P2Y2$^{-/-}$-tp mice challenged in a model of chronic inflammation due to high-fat diet feeding were not protected against adipose tissue inflammation or insulin resistance. However, a reduction in the formation of crown-like structures was observed in perigonadal adipose tissue from P2Y2$^{-/-}$-tp mice compared to WT-tp mice. Inflammatory macrophages assemble around dying adipocytes, forming what are termed CLSs [24]. As the number of macrophages increases in inflamed adipose tissue during expansion, usually the incidence of crown-like structure formation increases as well. This leads to a direct correlation of the number of CLS (which is also correlated with the number of macrophages) and body weight. Our data show that while the number of macrophages increases in P2Y2-deficient animals just like in wild type, this does not result in the formation of CLS. Therefore, we conclude that P2Y2 deficiency in macrophages may prevent CLS formation, while a correlation of macrophage numbers with body weight gain still persists. Chemokines like CCL2 recruit monocytes to adipose tissue [30]; however, little is known about how CLSs are formed. Recently, macrophage-inducible C-type lectin was shown to contribute to CLS formation and adipose tissue fibrosis [31], but there are likely to be multiple signaling events that contribute to CLS formation. Macrophages that form CLS are thought to be recruited to apoptotic adipocytes, and apoptotic cells have been shown to release ATP as a "find-me" signal for phagocytic cells [9]. Since extracellular ATP signaling through P2Y2 mediates macrophage chemotaxis [32], our data support a mechanism by which macrophage P2Y2 receptors may participate in the formation of CLS. Interestingly, the absence of CLS in high-fat fed P2Y2$^{-/-}$-tp mice did not appear to impact adipose tissue inflammation as mRNA levels of cytokines such as *Il6*, *Tnfα*, and *Il1β* were not significantly different between WT-tp and P2Y2$^{-/-}$-tp mice and had also no effect on the development of insulin resistance.

Together, we show here that P2Y2 receptors on myeloid cells are critically involved in regulating acute inflammatory responses both in vitro and in vivo. However, we found that myeloid P2Y2 receptors are dispensable for the development of diet-induced adipose

tissue inflammation and the development of insulin resistance in obese mice.

Funding information This study was supported by grants from the National Institutes of Health NIH-P01HL120840 (to NL). SEA was supported by an AHA predoctoral fellowship and by an NIH training grant (HL007284).

Compliance with ethical standards

Conflicts of interest Samantha E. Adamson declares that she has no conflict of interest.

Garren Montgomery declares that he has no conflict of interest.

Scott A. Seaman declares that he has no conflict of interest.

Shayn M. Peirce-Cottler declares that she has no conflict of interest.

Norbert Leitinger declares that he has no conflict of interest.

Ethical approval All animal studies were approved by the Animal Care and Use Committee at the University of Virginia.

References

1. Junger WG (2011) Immune cell regulation by autocrine purinergic signalling. Nat Rev Immunol 11:201–212
2. Eltzschig HK, Sitkovsky MV, Robson SC (2012) Purinergic signaling during inflammation. N Engl J Med 367:2322–2333
3. Cekic C, Linden J (2016) Purinergic regulation of the immune system. Nature reviews. Immunology 16:177–192
4. Inoue Y, Chen Y, Hirsh MI, Yip L, Junger WG (2007) A3 and P2Y2 receptors control the recruitment of neutrophils to the lungs in a mouse model of sepsis. Shock 1
5. Ayata CK, Ganal SC, Hockenjos B, Willim K, Vieira RP, Grimm M et al (2012) Purinergic P2Y2 receptors promote neutrophil infiltration and hepatocyte death in mice with acute liver injury. Gastroenterology 143:1620–1629.e4
6. Desai BN, Leitinger N (2014) Purinergic and calcium signaling in macrophage function and plasticity. Front Immunol 5:580
7. Eun SY, Seo J, Park SW, Lee JH, Chang KC, Kim HJ (2014) LPS potentiates nucleotide-induced inflammatory gene expression in macrophages via the upregulation of P2Y2 receptor. Int Immunopharmacol 18:270–276
8. Elliott MR, Chekeni FB, Trampont PC, Lazarowski ER, Kadl A, Walk SF et al (2009) Nucleotides released by apoptotic cells act as a find-me signal to promote phagocytic clearance. Nature 461:282–286
9. Chekeni FB, Elliott MR, Sandilos JK, Walk SF, Kinchen JM, Lazarowski ER et al (2010) Pannexin 1 channels mediate 'find-me' signal release and membrane permeability during apoptosis. Nature 467:863–867
10. Adamson SE, Leitinger N (2014) The role of pannexin1 in the induction and resolution of inflammation. FEBS Lett 588:1416–1422
11. Burnstock G, Pelleg A (2014) Cardiac purinergic signalling in health and disease. Purinergic Signal 11:1–46
12. Burnstock G, Novak I (2013) Purinergic signalling and diabetes. Purinergic Signal 9:307–324
13. Sun K, Kusminski CM, Scherer PE (2011) Adipose tissue remodeling and obesity. J Clin Investig 121:2094–2101
14. Weisberg SP, Hunter D, Huber R, Lemieux J, Slaymaker S, Vaddi K et al (2006) CCR2 modulates inflammatory and metabolic effects of high-fat feeding. J Clin Investig 116:115–124
15. Patsouris D, Li P, Thapar D, Chapman J, Olefsky JM, Neels JG (2008) Ablation of CD11c-positive cells normalizes insulin sensitivity in obese insulin resistant animals. Cell Metab 8:301–309
16. Stienstra R, van Diepen JA, Tack CJ, Zaki MH, van de Veerdonk FL, Perera D et al (2011) Inflammasome is a central player in the induction of obesity and insulin resistance. Proc Natl Acad Sci U S A 108:15324–15329
17. Vandanmagsar B, Youm YH, Ravussin A, Galgani JE, Stadler K, Mynatt RL et al (2011) The NLRP3 inflammasome instigates obesity-induced inflammation and insulin resistance. Nat Med 17:179–188
18. Sun S, Xia S, Ji Y, Kersten S, Qi L (2012) The ATP-P2X7 signaling axis is dispensable for obesity-associated inflammasome activation in adipose tissue. Diabetes 61:1471–1478
19. Meher AK, Sharma PR, Lira VA, Yamamoto M, Kensler TW, Yan Z et al (2012) Nrf2 deficiency in myeloid cells is not sufficient to protect mice from high-fat diet-induced adipose tissue inflammation and insulin resistance. Free Radic Biol Med 52:1708–1715
20. Linton MF, Atkinson JB, Fazio S (1995) Prevention of atherosclerosis in apolipoprotein E-deficient mice by bone marrow transplantation. Science (New York, NY) 267:1034–1037
21. Kadl A, Meher AK, Sharma PR, Lee MY, Doran AC, Johnstone SR et al (2010) Identification of a novel macrophage phenotype that develops in response to atherogenic phospholipids via Nrf2. Circ Res 107:737–746
22. Adamson SE, Griffiths R, Moravec R, Senthivinayagam S, Montgomery G, Chen W et al (2016) Disabled homolog 2 controls macrophage phenotypic polarization and adipose tissue inflammation. J Clin Invest 126:1311–1322
23. Ayala JE, Samuel VT, Morton GJ, Obici S, Croniger CM, Shulman GI et al (2010) Standard operating procedures for describing and performing metabolic tests of glucose homeostasis in mice. Dis Model Mech 3:525–534
24. Shaul ME, Bennett G, Strissel KJ, Greenberg AS, Obin MS (2010) Dynamic, M2-like remodeling phenotypes of CD11c+ adipose tissue macrophages during high-fat diet-induced obesity in mice. Diabetes 59:1171–1181
25. Wentworth JM, Naselli G, Brown WA, Doyle L, Phipson B, Smyth GK et al (2010) Pro-inflammatory CD11c+CD206+ adipose tissue macrophages are associated with insulin resistance in human obesity. Diabetes 59:1648–1656
26. Nishida M, Ogushi M, Suda R, Toyotaka M, Saiki S, Kitajima N et al (2011) Heterologous down-regulation of angiotensin type 1 receptors by purinergic P2Y2 receptor stimulation through S-nitrosylation of NF-kappaB. Proc Natl Acad Sci U S A 108:6662–6667
27. Thomas AC, Mattila JT (2014) "Of mice and men": arginine metabolism in macrophages. Front Immunol 5:479
28. Caldwell RB, Toque HA, Narayanan SP, Caldwell RW (2015) Arginase: an old enzyme with new tricks. Trends Pharmacol Sci 36:395–405
29. Kobayashi Y (2010) The regulatory role of nitric oxide in proinflammatory cytokine expression during the induction and resolution of inflammation. J Leukoc Biol 88:1157–1162
30. Kanda H (2006) MCP-1 contributes to macrophage infiltration into adipose tissue, insulin resistance, and hepatic steatosis in obesity. J Clin Investig 116:1494–1505
31. Tanaka M, Ikeda K, Suganami T, Komiya C, Ochi K, Shirakawa I et al (2014) Macrophage-inducible C-type lectin underlies obesity-induced adipose tissue fibrosis. Nat Commun 5:4982
32. Corriden R, Insel PA (2012) New insights regarding the regulation of chemotaxis by nucleotides, adenosine, and their receptors. Purinergic Signal 8:587–598